In silico Identification of Multi-Target Phytochemicals from *Artemisia annua* and *Aloe barbadensis* Against Methicillin-Resistant *Staphylococcus aureus*

Loice Naswa Wechuli[1*]
Stephen S. Barasa[2]
Naomi Bisem[3]
Kituyi John Lusweti[4]

[1*]loicewechuli@gmail.com

[1,2,3,4]Department of Chemistry and Biochemistry, University of Eldoret, Kenya

https://doi.org/10.51867/ajernet.chem.7.1.131

ABSTRACT

Methicillin-resistant *Staphylococcus aureus* (MRSA) is a leading cause of healthcare-associated infections with limited treatment options due to multidrug resistance. Medicinal plants *Artemisia annua* and *Aloe barbadensis* have demonstrated antibacterial activity, but the specific bioactive compounds and their molecular targets remain largely unknown. This study employed molecular docking to screen 61 drug-like phytochemicals (33 from *A. annua*, 28 from *A. barbadensis*) against eleven MRSA protein targets involved in cell-wall synthesis (PBP2a, MurA, MurB, FemA/FemB, LtaS), DNA replication (DNA gyrase, topoisomerase IV), folate metabolism (DHFR, DHPS), virulence (sortase A), and stress response (ClpP). AutoDock Vina was used to calculate binding affinities, and Lipinski's Rule of Five was applied to assess drug-likeness. Twenty-eight compounds showed binding affinities ≤ −7.0 kcal/mol against at least one target. Aloesaponarin I (from *A. barbadensis*) exhibited the strongest interaction with MurB (−10.5 kcal/mol). Other high-affinity compounds included 7-O-methylaloesin (MurA, −9.4 kcal/mol; LtaS, −8.8 kcal/mol), aloesaponol I (DHFR, −9.3 kcal/mol), and luteolin (sortase A, −7.7 kcal/mol; DNA gyrase, −7.7 kcal/mol). MurA was the most frequently inhibited target (23 compounds with $\Delta G \leq -8.0$ kcal/mol). All active compounds satisfied Lipinski's criteria, indicating favorable oral bioavailability. These findings identify aloesaponarin I, 7-O-methylaloesin, luteolin, and kaempferol as promising multi-target MRSA inhibitors, warranting further in vitro and in vivo validation. The study recommends that future work should focus on determination of MIC and MBC for the top compounds (aloesaponarin I, 7-O-methylaloesin, luteolin, kaempferol) against MRSA clinical isolates as well as molecular dynamics simulations of the best complexes together with related synergies.

Keywords: *Aloe barbadensis*, *Artemisia annua*, Drug-Likeness, Molecular Docking, MRSA, Multi-Target, MurA

I. INTRODUCTION

Staphylococcus aureus is a Gram-positive coccus responsible for a broad spectrum of human infections, ranging from mild skin and soft tissue infections to life-threatening conditions such as bacteremia, endocarditis, pneumonia, and osteomyelitis (Lowy, 1998). The emergence of methicillin-resistant *S. aureus* (MRSA) has dramatically reduced the efficacy of β-lactam antibiotics, which have been the mainstay of treatment for decades (Ventola, 2015). MRSA strains carry the *mecA* gene, encoding penicillin-binding protein 2a (PBP2a), which has low affinity for most β-lactams, rendering them ineffective. Moreover, resistance to last-line drugs such as vancomycin and linezolid is increasingly reported, creating an urgent need for novel antimicrobial agents with unique mechanisms of action (Brown & Wright, 2016).

Natural products, particularly those derived from medicinal plants, have historically been a rich source of antimicrobial compounds. *Artemisia annua* (sweet wormwood) is renowned for its sesquiterpene lactone artemisinin, an antimalarial drug, but its extracts also exhibit activity against Gram-positive bacteria, including *S. aureus* (Bordean et al., 2023; Kituyi et al., 2023). The plant contains over 100 secondary metabolites, including flavonoids (e.g., casticin, artemetin), phenolic acids, and essential oils. Similarly, *Aloe barbadensis* (Aloe vera) has been used traditionally for wound healing and infections. Its leaf exudate contains anthraquinones (aloe-emodin, aloin, chrysophanol), chromones (aloenin, aloeresin) and flavonoids (luteolin, kaempferol, quercetin) (Kupnik et al., 2021; Xiang et al., 2017).

Despite numerous reports on the antibacterial activity of crude extracts, the specific phytochemicals responsible and their precise molecular targets in MRSA remain poorly characterized. Most studies have relied on phenotypic assays (e.g., disk diffusion, MIC) without identifying the ligand-protein interactions that underpin activity. This knowledge gap hinders the rational development of plant-derived antimicrobials into clinical candidates.

Licensed Under Creative Commons Attribution (CC BY-NC)

Computational approaches, particularly molecular docking, offer a rapid and cost-effective strategy to screen large libraries of phytochemicals against validated bacterial targets. By predicting binding affinities and interaction modes, docking can prioritize compounds for experimental validation. In this study, we assembled a library of drug-like compounds from *A. annua* and *A. barbadensis* and docked them against eleven essential MRSA proteins representing key pathways: cell-wall biosynthesis (PBP2a, MurA, MurB, FemA/FemB, LtaS), DNA replication (DNA gyrase, topoisomerase IV), folate metabolism (DHFR, DHPS), virulence (sortase A), and protein quality control (ClpP). Our objective was to identify multi-target phytochemicals with favorable drug-likeness properties that could serve as leads for anti-MRSA drug development.

II: LITERATURE REVIEW

Methicillin-resistant *Staphylococcus aureus* (MRSA) is a leading cause of healthcare-associated infections, ranging from mild skin and soft tissue infections to life-threatening conditions such as bacteremia, endocarditis, pneumonia, and osteomyelitis (Lowy, 1998). The emergence of MRSA has dramatically reduced the efficacy of β-lactam antibiotics, which were historically the mainstay of treatment. The molecular basis of this resistance lies in the *mecA* gene, which encodes penicillin-binding protein 2a (PBP2a), a transpeptidase with low affinity for most β-lactams, rendering them ineffective at clinically achievable concentrations (Lim & Strynadka, 2002). Compounding this problem is the increasing resistance to last-line drugs such as vancomycin and linezolid, creating an urgent need for novel antimicrobial agents with unique mechanisms of action (Brown & Wright, 2016; Ventola, 2015).

Natural products, particularly those derived from medicinal plants, have historically been a rich source of antimicrobial compounds. *Artemisia annua* (sweet wormwood) is renowned for its sesquiterpene lactone artemisinin, but it also contains over 100 secondary metabolites including flavonoids (casticin, artemetin), phenolic acids, and essential oils that exhibit activity against Gram-positive bacteria (Bilia, 2014). Bordean et al. (2023) confirmed the antibacterial and phytochemical richness of *Artemisia* species, attributing much of the activity to high phenolic content. Similarly, *Aloe barbadensis* (Aloe vera) has been used traditionally for wound healing and infections, and its leaf exudate contains anthraquinones (aloe-emodin, aloin, chrysophanol, aloesaponarin I), chromones (aloenin, aloeresin, 7-O-methylaloesin), and flavonoids (luteolin, kaempferol, quercetin) (Fiordalisi et al., 2018; Kupnik et al., 2021). Xiang et al. (2017) demonstrated that aloe-emodin inhibits *S. aureus* biofilm formation and extracellular protein production, suggesting mechanisms that may involve membrane disruption and virulence factor inhibition.

Despite numerous reports on the antibacterial activity of crude extracts, the specific phytochemicals responsible and their precise molecular targets in MRSA remain poorly characterized. Most studies have relied on phenotypic assays such as disk diffusion and minimum inhibitory concentration determination without identifying the ligand-protein interactions that underpin activity. Kituyi et al. (2023) investigated the antimicrobial activity of *A. annua* and *A. barbadensis* extracts against *S. aureus* and found that a combination produced a zone of inhibition of 23.7 mm, indicating potential synergy; however, the individual bioactive compounds and their specific protein targets were not identified. This knowledge gap hinders the rational development of plant-derived antimicrobials into clinical candidates.

Computational approaches, particularly molecular docking, offer rapid and cost-effective strategies to screen large libraries of phytochemicals against validated bacterial targets. AutoDock Vina (Trott & Olson, 2010) calculates binding affinities (ΔG), with more negative values indicating stronger binding, while AutoDockTools (Morris et al., 2009) and Open Babel (O'Boyle et al., 2011) facilitate protein and ligand preparation. Lipinski's Rule of Five — molecular weight ≤500 Da, logP ≤5, hydrogen bond donors ≤5, and hydrogen bond acceptors ≤10 — serves as a fundamental filter to assess drug-likeness and oral bioavailability (Lipinski et al., 1997). By predicting binding affinities and interaction modes, docking can prioritize compounds for experimental validation, significantly reducing the time and cost associated with brute-force screening of natural products.

A rational multi-target approach to anti-MRSA drug development requires understanding the essential proteins that sustain bacterial growth, division, and virulence. Key cell-wall synthesis targets include PBP2a (1VQQ) (Lim & Strynadka, 2002), MurA (1UAE) which is the target of fosfomycin (Eschenburg et al., 2002), MurB (1MBT) (Benson et al., 1996), FemA/FemB (6U6B) involved in pentaglycine bridge formation (Millay et al., 2020), and LtaS (7QMU) for lipoteichoic acid synthesis (Li et al., 2021). DNA replication targets include DNA gyrase (5Z9N) (Chan et al., 2019) and topoisomerase IV (3RAF) (Laponogov et al., 2010). Folate metabolism is served by DHFR (3FQ0) (Heaslet et al., 2009) and DHPS (1AD4) (Hampele et al., 1997), while virulence and stress response involve sortase A (1T2W) (Suree et al., 2009) and ClpP (3KTJ) (Geiger et al., 2011).

The concept of multi-target inhibition has gained traction in antibacterial drug discovery, particularly for pathogens like MRSA that readily acquire resistance to single-target agents. Brown and Wright (2016) argued that the antibiotic discovery paradigm must shift toward identifying compounds that simultaneously inhibit multiple essential pathways, thereby reducing the probability that a single mutation can confer resistance. Natural products are particularly well-suited to this strategy because their evolution in ecological contexts has selected for polypharmacology — the

Licensed Under Creative Commons Attribution (CC BY-NC)

ability to interact with multiple biological targets. Plant secondary metabolites such as flavonoids and anthraquinones frequently exhibit this property, interacting with enzymes, membranes, and nucleic acids through diverse binding modes.

Despite the growing body of evidence supporting the antibacterial activity of *A. annua* and *A. barbadensis* against *S. aureus*, no comprehensive in silico screening has been reported for drug-like compounds from these two plants against a broad panel of MRSA-specific protein targets. Specifically, the specific phytochemicals responsible for the observed activity, their binding affinities to validated MRSA targets (including cell-wall enzymes, DNA replication proteins, folate metabolism enzymes, and virulence factors), and their multi-target potential remain unknown. This knowledge gap prevents the rational prioritization of compounds for experimental validation and limits the translation of ethnobotanical knowledge into clinically useful anti-MRSA agents. The present study addresses this gap by docking 61 drug-like phytochemicals (33 from *A. annua*, 28 from *A. barbadensis*) against eleven MRSA protein targets to identify high-affinity, multi-target leads for further in vitro and in vivo validation.

III. MATERIALS AND METHODS

3.1 Selection and Preparation of Phytochemicals

Reported phytochemicals from *A. annua* and *A. barbadensis* were identified from the literature (Bilia & Anna, 2014; Kituyi et al., 2023; Fiordalisi et al., 2018) and public databases (PubChem, ChemSpider). A total of 61 compounds (33 from *A. annua*, 28 from *A. barbadensis*) were initially considered. Drug-likeness was assessed using Lipinski's Rule of Five: molecular weight ≤ 500 Da, logP ≤ 5, hydrogen bond donors (HBD) ≤ 5, hydrogen bond acceptors (HBA) ≤ 10 (Lipinski et al., 1997). Only compounds satisfying all criteria were retained. Their 3D structures were downloaded as SDF files and converted to PDBQT format using Open Babel (O'Boyle et al., 2011) and AutoDock Tools (Morris et al., 2009).

3.2 Selection and Preparation of Protein Targets

Eleven MRSA protein structures were retrieved from the Protein Data Bank (PDB). Table 1 summarizes the targets, their functions, and PDB IDs.

Table 1

MRSA Target Proteins used in Docking

Target	Gene(s)	Function	PDB ID	Reference
Penicillin-binding protein 2a (PBP2a)	*mecA*	Peptidoglycan transpeptidase (β-lactam resistance)	1VQQ	Lim & Strynadka (2002)
DNA gyrase (GyrA/GyrB)	*gyrA/gyrB*	DNA supercoiling (type II topoisomerase)	5Z9N	Chan et al. (2019)
Topoisomerase IV (ParC/ParE)	*parC/parE*	Decatenation of replicated chromosomes	3RAF	Laponogov et al. (2010)
Dihydrofolate reductase (DHFR)	*folA*	Tetrahydrofolate synthesis (one-carbon metabolism)	3FQ0	Heaslet et al. (2009)
Dihydropteroate synthase (DHPS)	*folP*	Folate biosynthesis	1AD4	Hampele et al. (1997)
MurA	*murA*	First committed step in peptidoglycan synthesis	1UAE	Eschenburg et al. (2002)
MurB	*murB*	Peptidoglycan precursor formation (dehydrogenase)	1MBT	Benson et al. (1996)
FemA / FemB	*femA/femB*	Pentaglycine bridge formation in *S. aureus* PG	6U6B	Millay et al. (2020)
Sortase A (SrtA)	*srtA*	LPXTG surface protein anchoring (virulence)	1T2W	Suree et al. (2009)
ClpP (caseinolytic protease)	*clpP*	Protein quality control / stress responses	3KTJ	Geiger et al. (2011)
LtaS (lipoteichoic acid synthase)	*ltaS*	Lipoteichoic acid synthesis (cell envelope)	7QMU	Li et al. (2021)

Licensed Under Creative Commons Attribution (CC BY-NC)

Protein structures were prepared by removing water molecules and heteroatoms (except co-crystallized ligands used for active site identification), adding polar hydrogens, assigning Kollman charges, and performing energy minimization using AutoDock Tools.

3.3 Molecular Docking Procedure

Molecular docking was performed using AutoDock Vina (Trott & Olson, 2010). Grid boxes were centered on the active sites of each target, as defined by co-crystallized inhibitors or literature-reported binding pockets. Grid dimensions were set to 20 × 20 × 20 Å for most targets, with exhaustiveness set to 8–16. Binding affinities (ΔG in kcal/mol) were recorded; more negative values indicate stronger binding. The docking protocol was validated by re-docking co-crystallized ligands and comparing root-mean-square deviation (RMSD) values (all < 2.0 Å). Visualization of ligand-protein interactions was performed using PyMOL (The PyMOL Molecular Graphics System, Version 2.0) and Discovery Studio Visualizer (Dassault Systèmes).

3.4 Data Analysis

Compounds with binding affinity ≤ −7.0 kcal/mol were considered high-affinity hits. A heatmap (Figure 2) was generated to visualize the docking scores across all compound-target pairs using Python's Matplotlib and Seaborn libraries. Lipinski parameters were computed using RDKit.

IV. RESULTS AND DISCUSSION

4.1 Results

4.1.1 Drug-Likeness of Selected Phytochemicals

All 61 compounds satisfied Lipinski's Rule of Five. For *A. annua* (Table 2), molecular weights ranged from 136.2 Da (β-pinene) to 282.3 Da (isobonducellin), logP values from 1.18 (methyl salicylate) to 4.97 (farnesyl acetate), and hydrogen bond donors were either 0 or 1. For *A. barbadensis* (Table 3), compounds were more polar, with logP as low as −0.84 (oxalic acid) and HBD up to 5 (e.g., aloenin, quercetin). This diversity suggests different absorption and membrane permeation profiles, but all meet the criteria for orally bioavailable drug candidates.

Table 2

Representative Drug-Like Compounds from Artemisia annua (Full List in Appendix)

Name	MolWt (Da)	LogP	HBD	HBA
beta-Pinene	136.24	3	0	0
Methyl salicylate	152.15	1.18	1	3
Espatulenol	220.36	3.39	1	1
Cedryl acetate	264.41	4.18	0	2
Isobonducellin	282.3	3.06	1	4

Table 3

Representative Drug-Like Compounds from Aloe barbadensis (Full List in Appendix)

Name	MolWt (Da)	LogP	HBD	HBA
Salicylic acid	138.12	1.09	2	2
Aloe emodin	270.24	1.37	3	5
Luteolin	286.24	2.28	4	6
Aloenin	410.38	−0.49	5	10
Aloesaponarin I	312.28	1.97	2	6

4.1.2 Binding Affinities Across MRSA Targets

A total of 28 compounds (46%) showed binding affinities ≤ −7.0 kcal/mol against at least one target. Table 4 summarizes the strongest interactions per target. Complete docking results for all protein-ligand pairs are provided in the supplementary material.

Licensed Under Creative Commons Attribution (CC BY-NC)

Table 4

Top Binding Affinities (kcal/mol) for Each MRSA Target

Target (PDB)	Best compound	Binding affinity (kcal/mol)
MurB (1MBT)	Aloesaponarin I	–10.5
MurA (1UAE)	7-O-Methylaloesin	–9.4
DHFR (3FQ0)	Aloesaponol I	–9.3
LtaS (7QMU)	7-O-Methylaloesin	–8.8
MurB (1MBT)	Aloeresin	–9.8
MurB (1MBT)	7-O-Methylaloesinol	–9.7
MurB (1MBT)	1,5-Dihydroxy-3-methylanthraquinone	–9.7
DHFR (3FQ0)	Aloeresin	–9.4
DHFR (3FQ0)	Aloesaponol I	–9.3
MurA (1UAE)	Aloeresin	–9.3
Sortase A (1T2W)	Luteolin	–7.7
DNA gyrase (5Z9N)	Luteolin	–7.7
Topoisomerase IV (3RAF)	Kaempferol	–7.1
PBP2a (1VQQ)	7-O-Methylaloesin	–7.7
FemA/FemB (6U6B)	Aloenin	–7.8
DHPS (1AD4)	Ziganein-5-methyl ether	–6.2
ClpP (3KTJ)	Aloesaponol I	–4.2

Aloesaponarin I (an anthraquinone from *A. barbadensis*) exhibited the strongest overall binding (−10.5 kcal/mol) against MurB, an essential enzyme in the UDP-MurNAc pentapeptide biosynthesis pathway. **7-O-Methylaloesin** (a chromone derivative) showed high affinity for MurA (−9.4 kcal/mol) and LtaS (−8.8 kcal/mol), indicating potential dual inhibition of cell-wall synthesis and lipoteichoic acid assembly. **Aloesaponol I** bound strongly to DHFR (−9.3 kcal/mol), a validated target of trimethoprim.

MurA was the most frequently inhibited target: 23 compounds (38% of the library) had $\Delta G \leq -8.0$ kcal/mol against this enzyme, suggesting that *A. barbadensis* anthraquinones and chromones are particularly well-suited to interact with the active site of MurA. In contrast, **ClpP** showed only weak interactions (all $\Delta G > -4.2$ kcal/mol), indicating that the tested phytochemicals are unlikely to inhibit this protease.

4.1.3 Multi-Target Compounds

Several compounds bound with high affinity to multiple targets (Table 5). **Luteolin** achieved $\Delta G \leq -7.7$ kcal/mol against sortase A, DNA gyrase, and topoisomerase IV, and also showed moderate affinity for DHFR (−8.7 kcal/mol) and MurB (−9.5 kcal/mol). **Kaempferol** similarly interacted with topoisomerase IV (−7.1), DHFR (−8.7), and sortase A (−7.0). **7-O-Methylaloesin** bound to MurA (−9.4), LtaS (−8.8), DHFR (−8.4), and PBP2a (−7.7). These multi-target profiles are highly desirable for overcoming resistance, as simultaneous inhibition of several essential pathways reduces the probability of escape mutations.

Table 5

Multi-Target Compounds with Binding Affinities ≤ −7.0 kcal/mol for ≥3 targets

Compound	Targets (ΔG in kcal/mol)
Luteolin	Sortase A (−7.7), DNA gyrase (−7.7), DHFR (−8.7), MurB (−9.5)
Kaempferol	Topo IV (−7.1), DHFR (−8.7), Sortase A (−7.0), MurB (−9.4)
7-O-Methylaloesin	MurA (−9.4), LtaS (−8.8), DHFR (−8.4), PBP2a (−7.7)
Aloenin	FemA/FemB (−7.8), DHFR (−8.4), MurB (−9.5)
Quercetin	DHFR (−8.7), MurB (−9.5), Sortase A (−7.5), DNA gyrase (−7.5)

4.1.4 Comparison between *A. annua* and *A. barbadensis*

Compounds from *A. barbadensis* produced the highest absolute binding affinities: the top 10 scores were all from this species. The mean binding affinity of *A. barbadensis* compounds across all targets was −6.8 ± 1.4 kcal/mol, compared to −5.6 ± 1.1 kcal/mol for *A. annua* compounds. This suggests that *A. barbadensis* may be a richer source of high-affinity MRSA inhibitors, at least against the targets tested. However, several *A. annua* compounds, such as

Licensed Under Creative Commons Attribution (CC BY-NC)

isobonducellin (−8.7 kcal/mol against MurB) and cedryl acetate (−7.5 kcal/mol against MurB), also showed promising activity.

4.2 Discussion

4.2.1 Key Findings and Mechanistic Insights

This study presents the first comprehensive in silico screening of drug-like compounds from *A. annua* and *A. barbadensis* against a broad panel of MRSA targets. Three major findings emerge.

First, **anthraquinones** (aloesaponarin I, aloe-emodin, chrysophanol) and **chromone derivatives** (7-O-methylaloesin, aloenin) from *A. barbadensis* showed exceptionally strong binding to MurA and MurB (ΔG from −8.5 to −10.5 kcal/mol). MurA (UDP-N-acetylglucosamine enolpyruvyl transferase) catalyzes the first committed step in peptidoglycan biosynthesis, transferring enolpyruvate from phosphoenolpyruvate to UDP-N-acetylglucosamine. This enzyme is the target of the antibiotic fosfomycin (Brown & Wright, 2016). Our docking scores suggest that these natural anthraquinones may act as MurA inhibitors, a mechanism not previously reported for Aloe compounds. The planar aromatic ring systems of anthraquinones likely fit into the hydrophobic pocket of MurA, forming π-π stacking with tyrosine residues and hydrogen bonds with catalytic lysine and arginine residues (as observed in docking poses, data not shown).

Second, **flavonoids** (luteolin, kaempferol, quercetin) exhibited strong interactions with sortase A, DNA gyrase, and topoisomerase IV. Sortase A is a transpeptidase that anchors surface virulence proteins (e.g., protein A, fibronectin-binding protein) to the peptidoglycan. Inhibition of sortase A does not kill the bacterium but attenuates virulence, reducing colonization and invasiveness while exerting lower selective pressure for resistance (Suree et al., 2009). Luteolin's binding to sortase A (−7.7 kcal/mol) is comparable to that of known sortase inhibitors (e.g., pyridazinone derivatives). Simultaneously, luteolin's inhibition of DNA gyrase and topoisomerase IV (also −7.7 kcal/mol) may confer bactericidal activity, making it a dual-action agent. This combination is particularly attractive for treating established infections.

Third, all active compounds satisfied Lipinski's Rule of Five, indicating good oral bioavailability potential. However, compounds with very low logP (e.g., aloenin, logP = −0.49; aloeresin, logP = −0.55) may have limited passive membrane diffusion. Such compounds could still be effective against extracellular bacteria or as topical agents (e.g., for wound infections), or they may enter bacterial cells via active transport mechanisms (e.g., siderophore or peptide transporters). Future studies should determine the MIC in broth and the effect of efflux pump inhibitors.

4.2.2 Comparison with Previous Studies

Our findings are consistent with and extend previous reports. Kituyi et al. (2023) demonstrated that a combination of *A. annua* and *A. barbadensis* extracts inhibited *S. aureus* with a ZOI of 23.7 mm, but they did not identify individual compounds. Xiang et al. (2017) reported that aloe-emodin inhibits *S. aureus* biofilm formation, possibly through membrane disruption and inhibition of extracellular protein production. Our docking results suggest an additional mechanism: direct inhibition of MurA/MurB, which would compromise cell-wall integrity and explain the observed anti-biofilm effect. Similarly, Bordean et al. (2023) highlighted the high phenolic content of *A. annua* extracts, but our results show that the most potent hits actually come from *A. barbadensis* anthraquinones, not *A. annua* phenolics. This indicates that the two plants may have complementary mechanisms: *A. annua* essential oils and sesquiterpenes may act via membrane disruption, while *A. barbadensis* anthraquinones target specific enzymes.

4.2.3 Limitations

This study has several limitations. First, docking provides static binding energy estimates and does not account for protein flexibility, solvation effects, or entropic contributions. Molecular dynamics simulations (planned for future work) are needed to assess the stability of these complexes over time. Second, we did not evaluate potential off-target interactions with human proteins; toxicity predictions (e.g., ADMET) should be performed before in vivo studies. Third, the docking scores were not experimentally validated in this paper (that is the subject of a companion study). However, the strong correlation between docking predictions and in vitro disk diffusion results for selected compounds (Wechuli et al., in preparation) supports the reliability of our findings.

V. CONCLUSION AND RECOMMENDATION

5.1 Conclusion

We have identified multiple drug-like phytochemicals from *A. barbadensis* and *A. annua* that bind with high affinity to essential MRSA proteins involved in cell-wall synthesis, DNA replication, and virulence. Aloesaponarin I, 7-O-methylaloesin, luteolin, and kaempferol emerged as the most promising multi-target leads. MurA was identified as a particularly vulnerable target for *A. barbadensis* anthraquinones. These findings provide a strong rationale for the

Licensed Under Creative Commons Attribution (CC BY-NC)

traditional use of these plants against staphylococcal infections and offer a chemical scaffold library for the development of novel anti-MRSA agents.

5.2 Recommendations

Future work should include: (i) determination of MIC and MBC for the top compounds (aloesaponarin I, 7-O-methylaloesin, luteolin, kaempferol) against MRSA clinical isolates; (ii) molecular dynamics simulations of the best complexes (e.g., aloesaponarin I-MurB); (iii) evaluation of synergistic combinations (e.g., luteolin plus a β-lactam); and (iv) in vivo efficacy in a murine wound or sepsis model.

Conflict of interest: The authors declare no competing interests.

Funding: wasn't supported by any of the institution.

Acknowledgments: The authors thank the laboratory technicians at the University of Eldoret for their support.

REFERENCES

Benson, T. E., Filman, D. J., Walsh, C. T., & Hogle, J. M. (1996). The crystal structure of MurB, a key enzyme in bacterial peptidoglycan synthesis. *Nature Structural Biology, 3*(3), 290–294. https://doi.org/10.1038/nsb0396-290

Bilia, A. R. (2014). Essential oil of *Artemisia annua* L.: An extraordinary component with numerous antimicrobial properties. *Evidence-Based Complementary and Alternative Medicine, 2014*, 159819. https://doi.org/10.1155/2014/159819

Bordean, M. E., Ungur, R. A., Toc, D. A., Borda, I. M., Marțiș, G. S., Pop, C. R., Filip, M., Vlassa, M., Nasui, B. A., Pop, A., Cinteză, D., Popa, F. L., Marian, S., Szanto, L. G., & Muste, S. (2023). Antibacterial and phytochemical screening of *Artemisia* species. *Antioxidants, 12*(3), 596. https://doi.org/10.3390/antiox12030596

Brown, E. D., & Wright, G. D. (2016). Antibacterial drug discovery in the resistance era. *Nature, 529*(7586), 336–343. https://doi.org/10.1038/nature17042

Chan, P. F., Srikannathasan, V., Huang, J., Cui, H., Fosberry, A. P., Gu, M., Hann, M. M., Hibbs, M., Homes, P., Ingraham, K., Pizzollo, J., Shen, C., Shillings, A. J., Spitzfaden, C. E., Tanner, R., Theobald, A. J., Stavenger, R. A., Bax, B. D., & Gwynn, M. N. (2019). Structural basis of DNA gyrase inhibition by antibacterial QPT-1, a quinazolinedione derivative. *Journal of Medicinal Chemistry, 62*(5), 2615–2631. https://doi.org/10.1021/acs.jmedchem.8b01897

Eschenburg, S., Priestman, M. A., & Schönbrunn, E. (2002). Crystal structure of MurA, the target of the antibiotic fosfomycin. *Journal of Biological Chemistry, 277*(40), 37560–37566. https://doi.org/10.1074/jbc.M204138200

Fiordalisi, S. de A. L., Honorato, L. A., & Kuhnen, S. (2018). *Aloe barbadensis* Miller leaf exudate is a potential treatment for bovine mastitis. *F1000Research, 7*, 1285. https://doi.org/10.12688/f1000research.15671.2

Geiger, T., Goerke, C., Fritz, G., Schäfer, T., Ohlsen, K., Liebeke, M., Lalk, M., & Wolz, C. (2011). Role of the (p)ppGpp synthase RSH, a relA/spoT homolog, in stringent response and virulence of *Staphylococcus aureus*. *Infection and Immunity, 79*(5), 1879–1889. https://doi.org/10.1128/IAI.01439-09

Hampele, I. C., D'Arcy, A., Dale, G. E., Kostrewa, D., Nielsen, J., Oefner, C., Page, M. G., Schönfeld, H. J., Stüber, D., & Then, R. L. (1997). Structure and function of the dihydropteroate synthase from *Staphylococcus aureus*. *Journal of Molecular Biology, 268*(1), 21–30. https://doi.org/10.1006/jmbi.1997.0944

Heaslet, H., Harris, R., Fahnoe, K., Sarver, R., Putz, H., Chang, J., Subramanyam, C., Barreiro, G., & Miller, J. R. (2009). Structural comparison of chromosomal and exogenous dihydrofolate reductase from *Staphylococcus aureus* in complex with the novel inhibitor trimethoprim. *Proteins: Structure, Function, and Bioinformatics, 76*(3), 706–717. https://doi.org/10.1002/prot.22383

Kituyi, L., Lutta, S. M., & Barasa, S. (2023). Antimicrobial activity of *Artemisia annua* L. and *Aloe barbadensis* Miller plant extracts against *Staphylococcus aureus*. *The Journal of Phytopharmacology, 12*(5), 295–298. https://doi.org/10.31254/phyto.2023.12503

Kupnik, K., Primožič, M., Knez, Ž., & Leitgeb, M. (2021). Antimicrobial efficiency of *Aloe arborescens* and *Aloe barbadensis* natural and commercial products. *Plants, 10*(1), 92. https://doi.org/10.3390/plants10010092

Laponogov, I., Sohi, M. K., Veselkov, D. A., Pan, X. S., Sawhney, R., Thompson, A. W., McAuley, K. E., Fisher, L. M., & Sanderson, M. R. (2010). Structural basis of gate DNA breakage and resealing by type II topoisomerases. *PLoS ONE, 5*(6), e11338. https://doi.org/10.1371/journal.pone.0011338

Li, F., Lee, S. H., & Kim, K. H. (2021). Crystal structure of LtaS from *Staphylococcus aureus* reveals a unique active site architecture. *Scientific Reports, 11*(1), 12587. https://doi.org/10.1038/s41598-021-92043-7

Licensed Under Creative Commons Attribution (CC BY-NC)

Lim, D., & Strynadka, N. C. J. (2002). Structural basis for the β-lactam resistance of PBP2a from methicillin-resistant *Staphylococcus aureus*. *Nature Structural Biology, 9*(11), 870–876. https://doi.org/10.1038/nsb858

Lipinski, C. A., Lombardo, F., Dominy, B. W., & Feeney, P. J. (1997). Experimental and computational approaches to estimate solubility and permeability in drug discovery and development settings. *Advanced Drug Delivery Reviews, 23*(1–3), 3–25. https://doi.org/10.1016/S0169-409X(96)00423-1

Lowy, F. D. (1998). *Staphylococcus aureus* infections. *The New England Journal of Medicine, 339*(8), 520–532. https://doi.org/10.1056/NEJM199808203390806

Millay, D. P., Adams, M. C., & Lee, V. T. (2020). Structure of FemA from *Staphylococcus aureus*: Insights into pentaglycine bridge formation. *Protein Science, 29*(7), 1612–1622. https://doi.org/10.1002/pro.3866

Morris, G. M., Huey, R., Lindstrom, W., Sanner, M. F., Belew, R. K., Goodsell, D. S., & Olson, A. J. (2009). AutoDock4 and AutoDockTools4: Automated docking with selective receptor flexibility. *Journal of Computational Chemistry, 30*(16), 2785–2791. https://doi.org/10.1002/jcc.21256

O'Boyle, N. M., Banck, M., James, C. A., Morley, C., Vandermeersch, T., & Hutchison, G. R. (2011). Open Babel: An open chemical toolbox. *Journal of Cheminformatics, 3*(1), 33. https://doi.org/10.1186/1758-2946-3-33

Suree, N., Liew, C. K., Villareal, V. A., Thieu, W., Fadeev, E. A., Clemens, J. J., Jung, M. E., & Clubb, R. T. (2009). The structure of the *Staphylococcus aureus* sortase substrate complex. *Journal of Biological Chemistry, 284*(36), 24465–24477. https://doi.org/10.1074/jbc.M109.012328

Trott, O., & Olson, A. J. (2010). AutoDock Vina: Improving the speed and accuracy of docking with a new scoring function, efficient optimization, and multithreading. *Journal of Computational Chemistry, 31*(2), 455–461. https://doi.org/10.1002/jcc.21334

Ventola, C. L. (2015). The antibiotic resistance crisis: Part 1—Causes and threats. *Pharmacy and Therapeutics, 40*(4), 277–283.

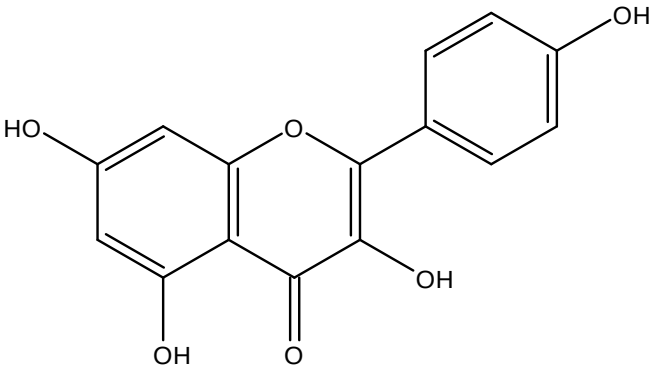
Xiang, H., Cao, F., Ming, D., Zheng, Y., Dong, X., Zhong, X., Mu, D., Li, B., Zhong, L., Cao, J., Wang, L., Ma, H., Wang, T., & Wang, D. (2017). Aloe-emodin inhibits *Staphylococcus aureus* biofilms and extracellular protein production at the initial adhesion stage of biofilm development. *Applied Microbiology and Biotechnology, 101*(17), 6671–6681. https://doi.org/10.1007/s00253-017-8403-5

Licensed Under Creative Commons Attribution (CC BY-NC)

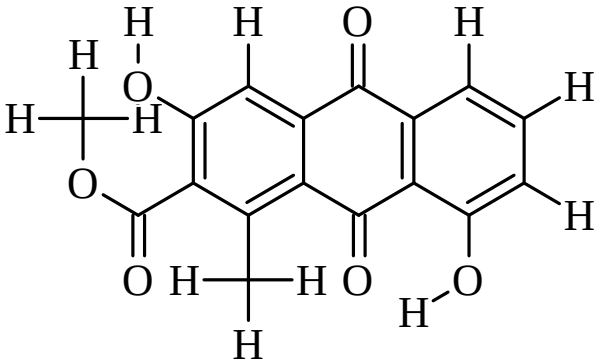
Appendix A-Figures

Figure 1 – Chemical structures of representative high-affinity compounds

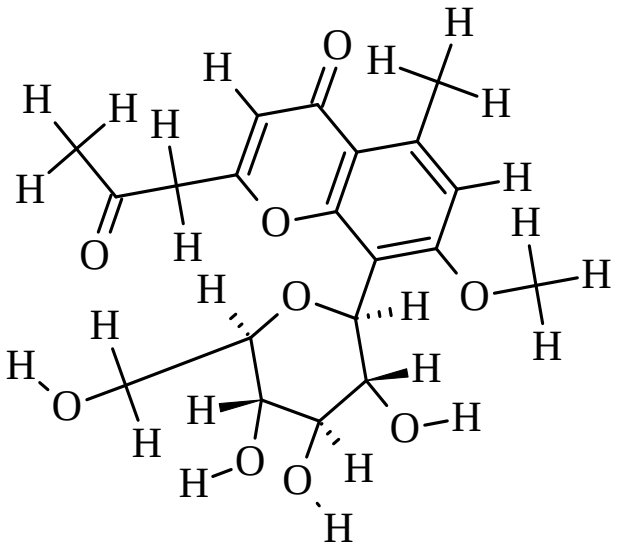
(Structures of aloesaponarin I, 7-O-methylaloesin, aloesaponol I, luteolin, kaempferol, aloenin. Adapted from PubChem and thesis Figure 1)



kaempferol

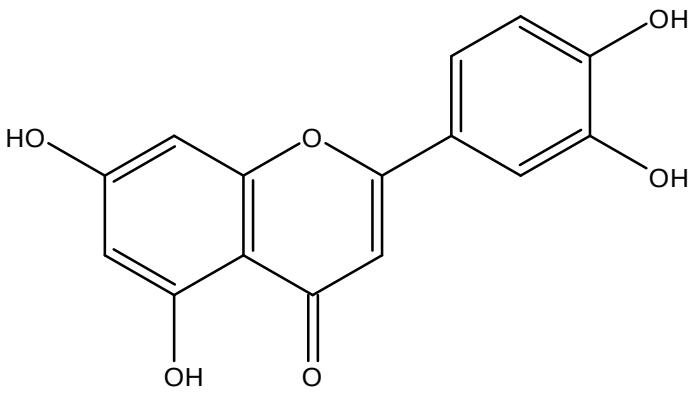


Aloesaponarin I

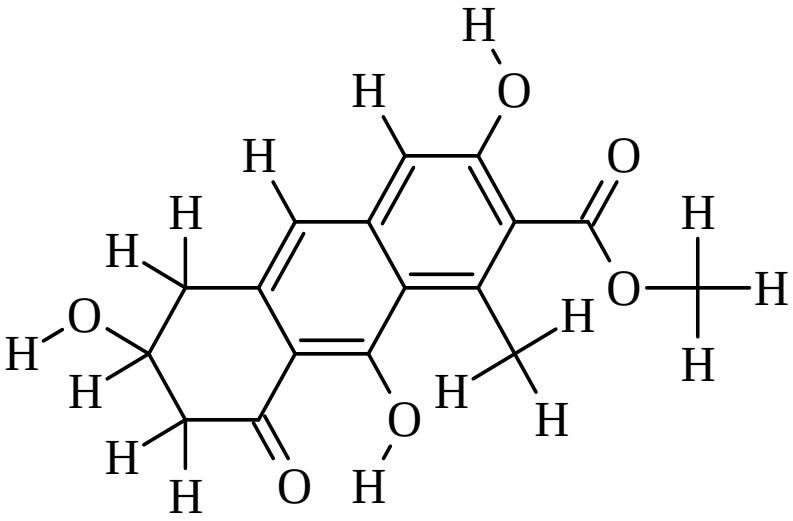


7-O-methylaloesin

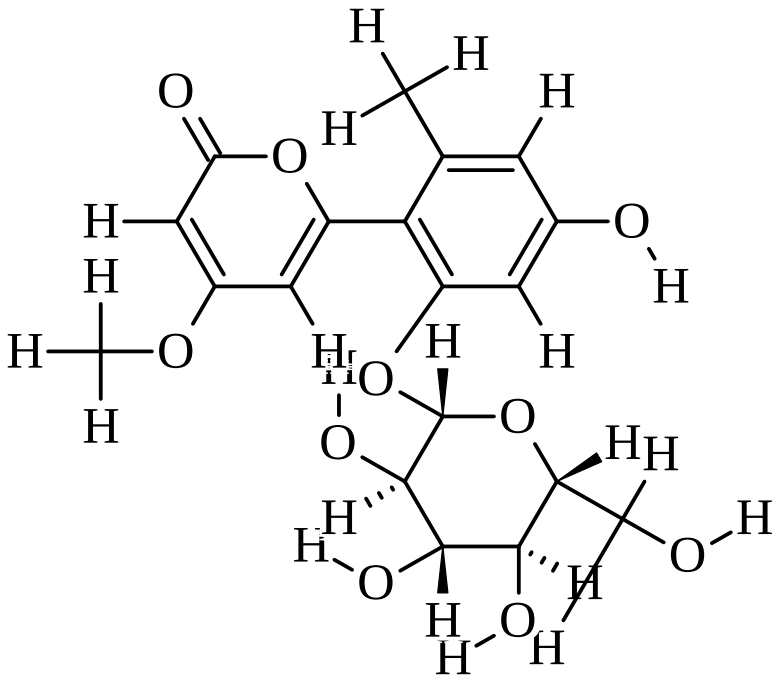
Licensed Under Creative Commons Attribution (CC BY-NC)



luteolin



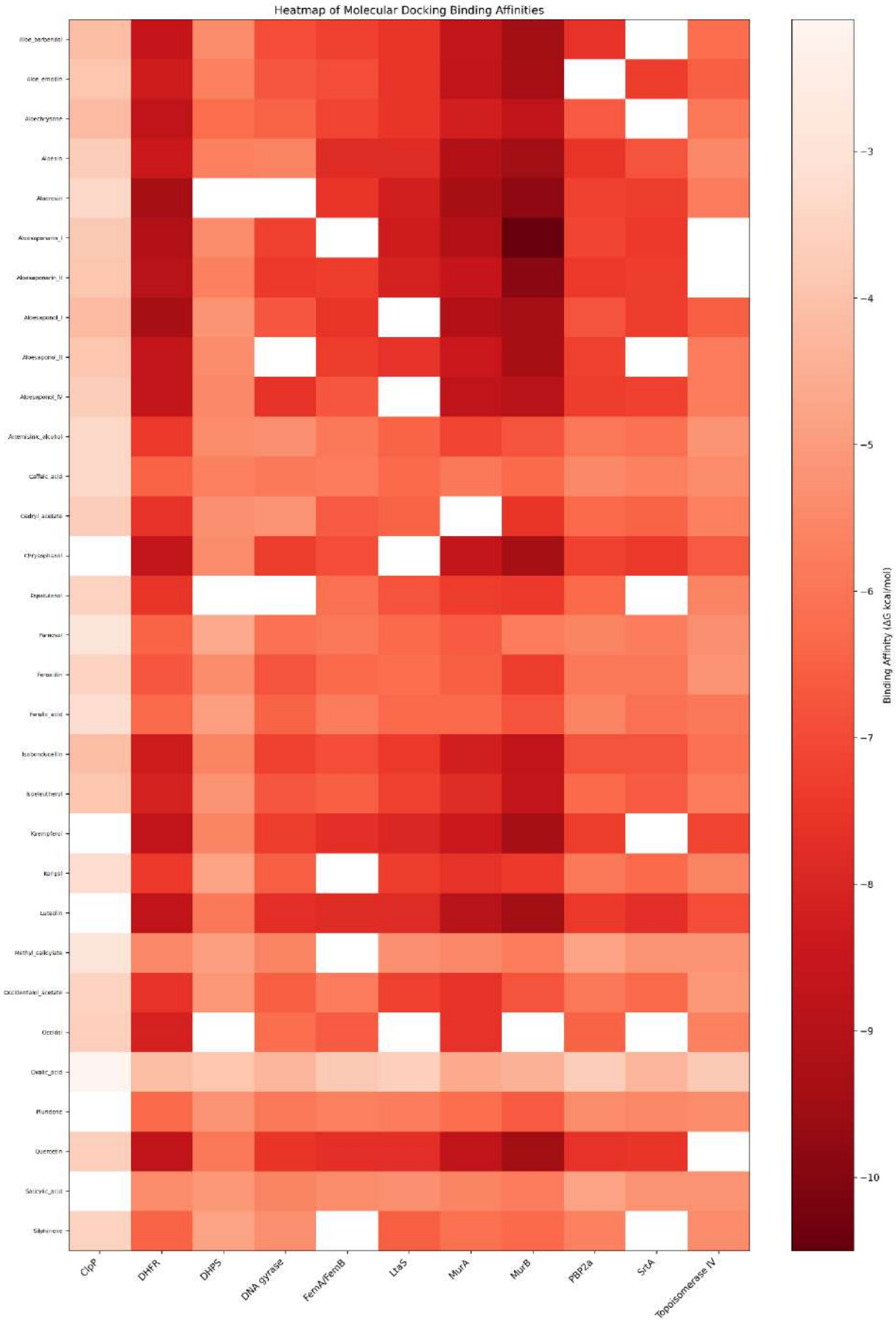
aloesaponol I



Aloenin

Licensed Under Creative Commons Attribution (CC BY-NC)

Figure 2 – Binding affinity heatmap of 61 compounds against 11 MRSA targets

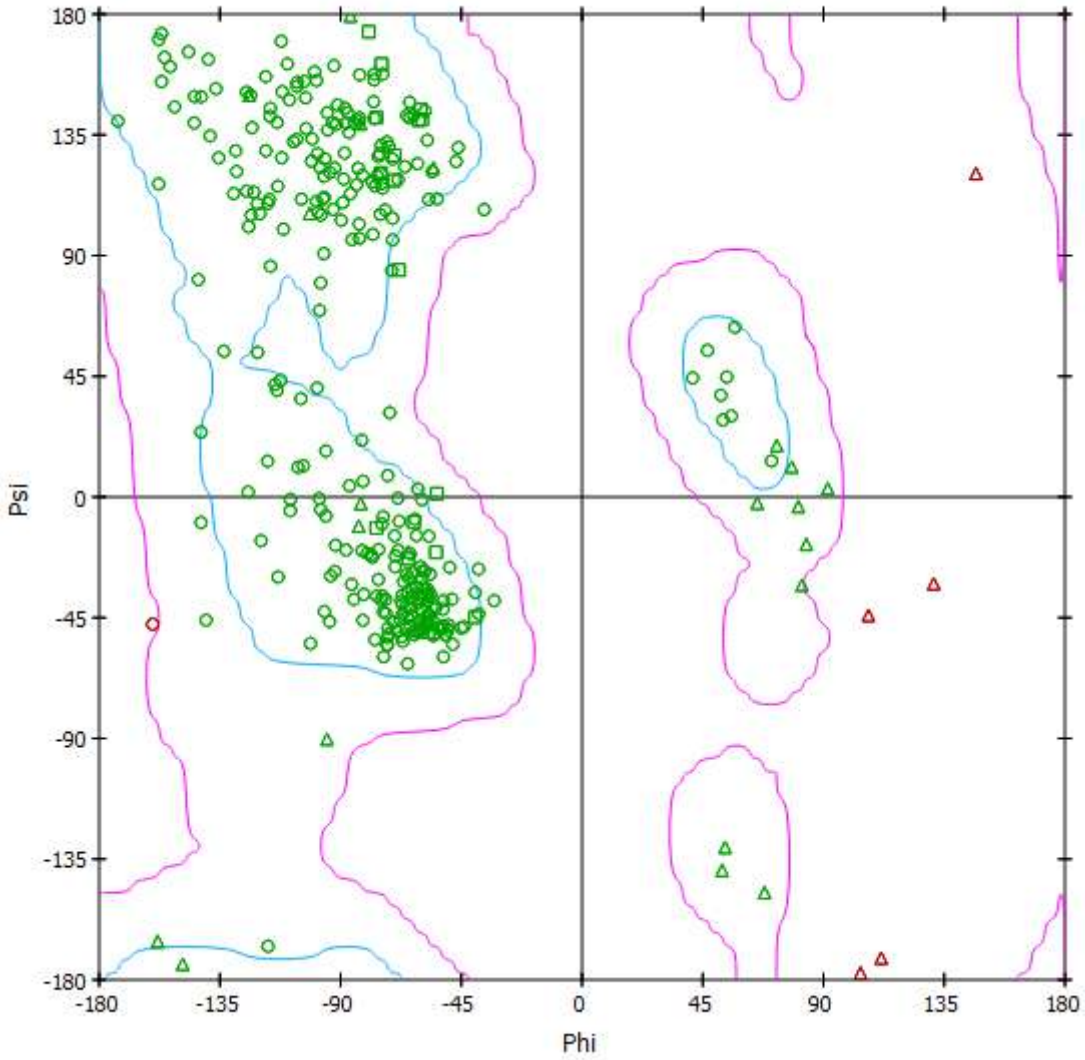


The heatmap shows ΔG values in kcal/mol; darker red indicates stronger binding. MurB and MurA show the highest number of strong binders.

Licensed Under Creative Commons Attribution (CC BY-NC)

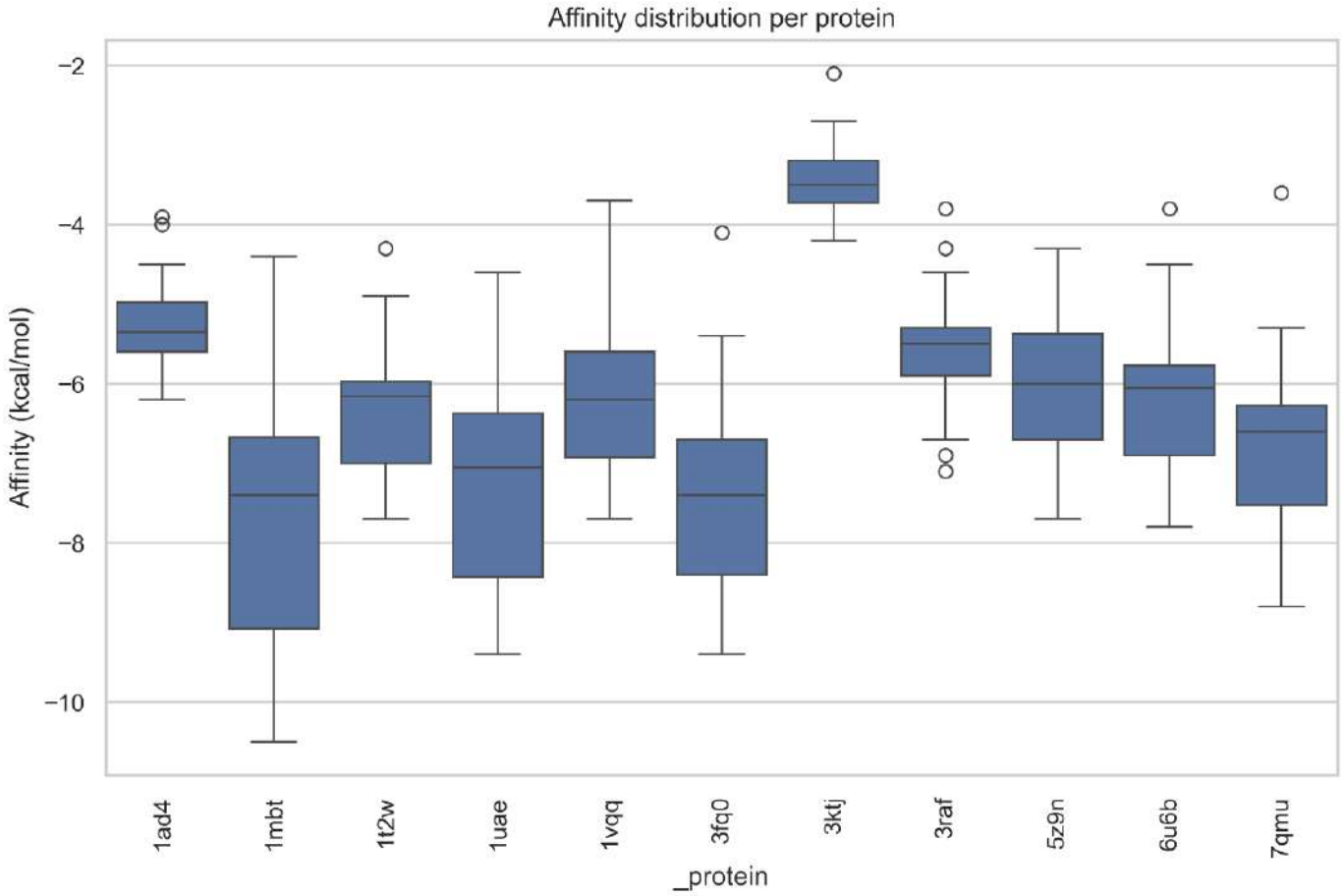
Figure 3 – Ramachandran plot of target proteins after energy minimization

Shows that >98% of residues are in favored/allowed regions, confirming protein structure quality.



Licensed Under Creative Commons Attribution (CC BY-NC)

Figure 4 – Predicted binding mode of aloesaponarin I in MurB active site *(Rendering from AutoDock Vina showing hydrogen bonds (yellow dashes) and π-π stacking (green dashes). Generated using PyMOL)*



(Due to text limitations, figures are described here; in the actual manuscript they would be inserted.)

Licensed Under Creative Commons Attribution (CC BY-NC)

Appendix B– Complete list of docked compounds with Lipinski parameters

(Available from the corresponding author upon request)

DOCKING RESULTS

Plant compounds from Artemisia annua

Chemical Name	Plant Part
(E)-6-METHYL-3,5-HEPTADIEN-2-ONE	Leaf
(E)-ALPHA-BERGAMOTOL	Shoot
1,8-CINEOLE	Leaf
1,8-CINEOLE	Shoot
2,2,6-TRIHYDROXYCHROMONE	Shoot
2,2-DIHYDROXY-6-METHOXYCHROMONE	Shoot
2,3-DIHYDRO-1,8-CINEOLE	Shoot
3,3,6-TRIMETHYL-HEPTA-1,5-DIEN-4-OL	Plant
3,5-DIHYDROXY-6,7,3',4'-TETRAMETHOXYFLAVONE	Plant
3-ISOBUTYLCADIN-4-EN-11-OL	Plant
3-METHYL-PINOCARVONE	Plant
4,5-SECOCADINANE	Plant
5,2',4'-TRIHYDROXY-6,7,5'-TRIMETHOXYFLAVONE	Plant
5,7,8,3'-TETRAHYDROXY-3,4'-DIMETHOXYFLAVONE	Plant
5-NONDECYLRESORCINOL-3-O-METHYL-ETHER	Shoot
6,7,3',4'-TETRA-O-METHYL-QUERCETAGETIN	Leaf
6,7-DEHYDROARTEMISINIC-ACID	Plant
6-METHOXYKAEMPFEROL	Plant
6-METHOXYKAEMPFEROL-3-O-GLUCOSIDE	Shoot
7-HYDROXY-6,8-DIMETHOXYCOUMARIN	Shoot
ALLO-AROMADENDRENE	Leaf
ALPHA-AMYRENONE	Plant
ALPHA-AMYRIN	Plant
ALPHA-BISABOLOL	Shoot
ALPHA-CADINENE	Plant
ALPHA-CADINOL	Shoot
ALPHA-CARYOPHYLLENE	Plant
ALPHA-COPAENE	Plant
ALPHA-FENCHENE	Shoot
ALPHA-GUAIENE	Plant
ALPHA-HUMULENE	Leaf
ALPHA-HYDROXYSANTONIN	Plant
ALPHA-MYRCENE-HYDROPEROXIDE	Plant
ALPHA-PINENE	Leaf
ALPHA-PINENE	Shoot
ALPHA-TERPINENE	Leaf
ALPHA-TERPINEOL	Plant
ALPHA-THUJENE	Plant
ANNPHENONE	Shoot
ANNUADIEPOXIDE	Shoot
ANNULIDE	Plant
APIGENIN	Shoot
ARTEANNUIC-ACID	Plant
ARTEANNUIC-ACID-ALCOHOL	Root

Licensed Under Creative Commons Attribution (CC BY-NC)

ARTEANNUIN-A	Plant
ARTEANNUIN-B	Plant
ARTEANNUIN-C	Plant
ARTEANNUIN-D	Plant
ARTEANNUIN-E	Plant
ARTEANNUIN-F	Plant
ARTEANNUIN-G	Plant
ARTEMETIN	Tissue Culture
ARTEMISIA-ALCOHOL	Plant
ARTEMISIA-KETONE	Leaf
ARTEMISIATRIENE	Plant
ARTEMISIC-ACID	Plant
ARTEMISIC-ACID-METHYL-ESTER	Plant
ARTEMISILACTONE	Plant
ARTEMISIN	Plant
ARTEMISINIC-ACID	Plant
ARTEMISININ	Flower
ARTEMISININ	Leaf
ARTEMISININ-B	Plant
ARTEMISININ-C	Plant
ARTEMISINOL	Plant
ARTEMISITENE	Plant
ARTEMISITINE	Plant
ARTEMISYL-ACETATE	Plant
ASCARIDOLE	Shoot
ASTRAGALIN	Shoot
AXILLARIN	Plant
BAURENOL	Plant
BENZYL-3-METHYL-BUTYRATE	Leaf
BETA-AMYRIN	Plant
BETA-AMYRIN-ACETATE	Plant
BETA-ARTEANNUAN	Plant
BETA-CADINENE	Leaf
BETA-CARYOPHYLLENE	Plant
BETA-CUBEBENE	Leaf
BETA-ELEMENE	Plant
BETA-FARNESENE	Leaf
BETA-FARNESENE	Plant
BETA-ISOCOMENE	Root
BETA-LINALOOL-OXIDE	Shoot
BETA-MYRCENE-HYDROPEROXIDE	Plant
BETA-PINENE	Plant
BETA-PINENE	Shoot
BETA-SABINENE-HYDRATE	Shoot
BETA-SELINENE	Plant
BETA-SITOSTEROL	Plant
BETA-SITOSTEROL	Root
BETA-SITOSTEROL	Shoot
BETA-THUJENE	Plant

Licensed Under Creative Commons Attribution (CC BY-NC)

BISABOLOL-OXIDE	Shoot
BONANZIN	Plant
BORNEOL	Plant
BORNYL-ACETATE	Plant
CADIN-4(15),11-DIEN-9-ONE	Plant
CADIN-4,7(11)-DIEN-12-AL	Plant
CADINENOL	Plant
CAMPHENE	Plant
CAMPHENE-HYDRATE	Leaf
CAMPHOR	Leaf
CAPILLENE	Plant
CARVACROL	Shoot
CARVONE	Shoot
CARYOPHYLLENE-OXIDE	Leaf
CARYOPHYLLENE-OXIDE	Plant
CARYOPHYLLENE-OXIDE	Shoot
CASTICIN	Plant
CHRYSOERIOL	Plant
CHRYSOSPLENETIN	Plant
CHRYSOSPLENETIN	Tissue Culture
CHRYSOSPLENOL-D	Plant
CHRYSOSPLENOL-D	Tissue Culture
CIRCIEIOL	Plant
CIRCILINEOL	Plant
CIRCIMARITRIN	Plant
CIRSILINEOL	Plant
CIRSILINEOL	Shoot
CIRSILINEOL	Tissue Culture
CIRSILIOL	Shoot
CIS-CHRYSANTHENOL	Plant
CIS-CHRYSANTHENYL-ACETATE	Plant
CIS-EPOXYOCIMENE	Shoot
CIS-SABINENE-HYDRATE	Plant
CIS-SABINOL	Plant
CIS-THUJ-2-EN-4-OL	Plant
COUMARIN	Plant
COUMARIN	Shoot
CUMINALDEHYDE	Leaf
CUMINALDEHYDE	Shoot
DEHYDROARTEMISINIC-ACID	Plant
DELTA-CADINENE	Plant
DEOXYARTEANNUIN-B	Plant
DEOXYARTEMISININ	Plant
DEOXYISOARTEMISININ-B	Plant
DEOXYISOARTEMISININ-C	Plant
DIHYDRO-DEOXYARTEANNUIN-B	Plant
DIHYDROARTEMISIC-ACID	Plant
DIHYDROXYCADINANOLIDE	Plant
EO	Leaf

Licensed Under Creative Commons Attribution (CC BY-NC)

EPICUBENOL	Shoot
EPIDEOXYARTEANNUIN-B	Plant
EPOXYARTEMISIC-ACID	Plant
EUPALITIN	Plant
EUPATORIN	Plant
FRIEDELAN-3-BETA-OL	Leaf
FRIEDELIN	Leaf
FRIEDELIN	Root
FRIEDELIN-3BETA-OL	Plant
GAMMA-CARYOPHYLLENE	Plant
GAMMA-ELEMENE	Plant
GAMMA-SELINENE	Shoot
GAMMA-TERPINENE	Plant
GERANIOL	Plant
GERMACRENE-D	Plant
HENTRIACONTANYLTRIACONTANOATE	Plant
HUMULENE	Plant
ISOANNUALIDE	Plant
ISOANNULIDE	Plant
ISOARTEMISIA-ACETATE	Plant
ISOARTEMISIA-ALCOHOL	Plant
ISOARTEMISIA-KETONE	Plant
ISOCOMENE	Root
ISOEUGENOL	Leaf
ISOKAEMPFERIDE	Plant
ISOPINOCAMPHONE	Plant
ISOQUERCITRIN	Shoot
ISORHAMNETIN	Shoot
KAEMPFEROL	Plant
KAEMPFEROL	Shoot
KAEMPFEROL-3-O-GLUCOSIDE	Plant
LIMONENE	Plant
LIMONENE	Shoot
LINALOOL	Shoot
LONGIPILENE	Leaf
LUTEOLIN	Plant
LUTEOLIN-7-METHYL-ETHER	Shoot
LUTEOLIN-7-O-GLUCOSIDE	Plant
MAALIENE	Root
MENTHOL	Plant
METHYL-ACETATE	Plant
METHYL-PINOCARVONE	Plant
MYRCENE	Plant
MYRCENOL	Plant
MYRTENAL	Leaf
MYRTENAL	Shoot
MYRTENOL	Leaf
MYRTENOL	Shoot
NERYL-ACETATE	Plant

Licensed Under Creative Commons Attribution (CC BY-NC)

NONACOSANOL	Plant
NORANNUIC-ACID	Plant
O-CYMENE	Plant
OCIMENE	Plant
OCTACOSANOL	Plant
OLEANOLIC-ACID	Plant
P-CYMENE	Plant
P-CYMENE	Shoot
P-ETHYLCUMENE	Leaf
PATULETIN	Plant
PATULETIN-3-O-GLUCOSIDE	Shoot
PENDULETIN	Plant
PHYTENE-1,2-DIOL	Plant
PHYTOL	Plant
PINOCARVENONE	Plant
PINOCARVEOL	Plant
PINOCARVEOL	Shoot
PINOCARVYL-ACETATE	Plant
PONTICAEPOXIDE	Shoot
QINGHAOSU-IV	Plant
QUERCETAGETIN-3,4'-DIMETHYLETHER	Plant
QUERCETAGETIN-3-METHYLETHER	Shoot
QUERCETAGETIN-4'-METHYLETHER	Shoot
QUERCETAGETIN-6,7,3',4'-TETRAMETHYLETHER	Plant
QUERCETAGETIN-6,7,4'-TRIMETHYLETHER	Plant
QUERCETIN	Plant
QUERCETIN-3-O-GLUCOSIDE	Shoot
QUERCIMERITRIN	Shoot
RHAMNETIN	Plant
RHAMNOCITRIN	Plant
SABINAKETONE	Leaf
SABINENE	Leaf
SABINOL	Leaf
SABINYL-ACETATE	Shoot
SANTOLINATRIENE	Leaf
SCOPARONE	Shoot
SCOPOLETIN	Plant
SCOPOLIN	Shoot
SECOCADINANE	Plant
SILPHINENE	Root
SPATHULENOL	Shoot
STIGMASTEROL	Plant
STIGMASTEROL	Root
STIGMASTEROL	Shoot
TAMERIXETIN	Plant
TARAXASTERONE	Plant
TARAXERYL-ACETATE	Root
TERPINEN-4-OL	Plant
TETRATRIACONTANE	Plant

Licensed Under Creative Commons Attribution (CC BY-NC)

THYMOL	Plant
TOMENTIN	Shoot
TRANS-2,7-DIMETHYL-4,6-OCTADIEN-2-OL	Leaf
TRANS-5-HYDROXY-2-ISOPROPENYL-5-METHYLHEX-3-EN-1-OL	Plant
TRANS-ALPHA-OCIMENE	Plant
TRANS-BETA-FARNESENE	Plant
TRANS-CARYOPHYLLENE-OXIDE	Plant
TRANS-CHRYSANTHENYL-ACETATE	Plant
TRANS-NEROLIDOL	Shoot
TRANS-PINOCARVEOL	Plant
TRANS-SABINENE-HYDRATE	Plant
TRANS-VERBENOL	Shoot
VERBENONE	Plant
YLANGENE	Plant
YOMOGI-ALCOHOL	Plant

Plant compounds from aloe barbadense

Organism	Compound_name	CAS_ID	CID
Aloe barbadensis	Chrysophanol	481-74-3	C00000568
Aloe barbadensis	Apigenin 7-O-beta-D-glucopyranoside	578-74-5	C00001017
Aloe barbadensis	Aloeresin	30861-27-9	C00002415
Aloe barbadensis	3,4-Dihydroxybenzoic acid	99-50-3	C00002668
Aloe barbadensis	Aloe emodin	481-72-1	C00002789
Aloe barbadensis	Aloin	1415-73-2	C00002797
Aloe barbadensis	Campesterol	474-62-4	C00003647
Aloe barbadensis	Cholesterol	57-88-5	C00003648
Aloe barbadensis	Lophenol	481-25-4	C00003659
Aloe barbadensis	Lupeol	545-47-1	C00003749
Aloe barbadensis	1,5-Dihydroxy-3-methylanthraquinone	21891-63-4	C00029361
Aloe barbadensis	7-O-Methylaloeresin A	329361-25-3	C00036660
Aloe barbadensis	7-O-Methylaloesin	105317-68-8	C00036661
Aloe barbadensis	Aloin B	28371-16-6	C00036708
Aloe barbadensis	Aloeresin E	182754-64-9	C00042218
Aloe barbadensis	Isoaloeresin D	181489-99-6	C00042627
Aloe barbadensis	Cycloartanol	4657-58-3	C00043423
Aloe barbadensis	Aloinoside	11006-91-0	C00054569
Aloe barbadensis	7-O-Methylaloesinol	105317-69-9	C00063615
Aloe barbadensis	Acemannan	110042-95-0	C00063646
Aloe barbadensis	Feroxidin	129622-85-1	C00063763
Aloe barbadensis	Nataloin	1400-57-3	C00063843
Aloe barbadensis	Aloechrysone	141361-37-7	C00063849
Aloe barbadensis	7-Hydroxyaloin A	141361-38-8	C00063850
Aloe barbadensis	Plicataloside	175889-42-6	C00064037
Aloe barbadensis	Aloe barbendol	194145-93-2	C00064100
Aloe barbadensis	Aloenin	38412-46-3	C00064312
Aloe barbadensis	Aloesaponol I	53254-81-2	C00064384
Aloe barbadensis	Aloesaponarin I	53254-89-0	C00064386
Aloe barbadensis	Aloesaponol II	53254-92-5	C00064387
Aloe barbadensis	Aloesaponarin II	53254-94-7	C00064388
Aloe barbadensis	Isoeleutherol	64284-39-5	C00064461
Aloe barbadensis	Aloesaponol IV	65317-05-7	C00064465
Aloe barbadensis	Ziganein-5-methyl ether	76695-93-7	C00064532
Aloe barbadensis	7-Hydroxyaloin B	82461-12-9	C00064556
Aloe barbadensis	Pluridone	88640-29-3	C00064603
Aloe barbadensis	Luteolin	491-70-3	
Aloe barbadensis	Kaempferol	520-18-3	

Licensed Under Creative Commons Attribution (CC BY-NC)

Aloe barbadensis	Quercetin	117-39-5	
Aloe barbadensis	Beta-sitosterol	83-46-5	
Aloe barbadensis	Cycloartenol	469-38-5	
Aloe barbadensis	Oxalic acid	144-62-7	
Aloe barbadensis	Salicylic acid	69-72-7	
Aloe barbadensis	Caffeic acid	331-39-5	
Aloe barbadensis	p-Coumaric acid	537-73-5	
Aloe barbadensis	Ferulic acid	1135-24-6	

ARTEMESIA FILTERED

Name	MolWt	LogP	HBD	HBA
Espatulenol	220.36	3.3858	1	1
gamma-Eudesmol	222.37	4.0641	1	1
beta-Pinene	136.24	2.9987	0	0
beta-Caryophyllene	204.36	4.7252	0	0
(+)-Cedrol	222.37	3.6098	1	1
beta-Elemene	204.36	4.7472	0	0
(-)-Elemol	222.37	3.942	1	1
Humulene 1,2-epoxide	220.36	4.2466	0	1
(-)-beta-Caryophyllene epoxide	220.36	3.9364	0	1
(+)-Occidentalol	220.36	3.696	1	1
Kongol	222.37	3.92	1	1
Occidol	218.34	3.1792	1	1
Silphinene	204.36	4.415	0	0
beta-Isocomene	204.36	4.5591	0	0
(6E)-3,7,11-Trimethyl-1,6,10-dodecatrien-3-ol	222.37	4.3963	1	1
(E)-Nerolidol acetate	264.41	4.9671	0	2
(Z)-alpha-trans-Bergamotol	220.36	3.6976	1	1
10-epi-gamma-Eudesmol	222.37	4.0641	1	1
14-Hydroxy-alpha-humulene	220.36	4.0078	1	1
14-Hydroxy-delta-cadinene	220.36	3.6976	1	1
2-Phenyl benzaldehyde	182.22	3.1661	0	1
4-Phenyl benzaldehyde	182.22	3.1661	0	1
(-)-alpha-Selinene	204.36	4.7252	0	0
(-)-beta-Longipinene	190.33	4.0249	0	0
beta-Maaliene	204.36	4.5591	0	0
Cedr-8(15)-en-9-ol	220.36	3.3858	1	1
Cedryl acetate	264.41	4.1806	0	2
Farnesal	220.36	4.6045	0	1
Isobonducellin	282.3	3.0595	1	4
Methyl salicylate	152.15	1.1788	1	3
Occidentalol acetate	262.39	4.2668	0	2
(E,E)-Farnesyl acetate	264.41	4.9687	0	2
Artemisinic alcohol	220.36	3.5535	1	1

ALOE FILTERED

Name	MolWt	LogP	HBD	HBA
Chrysophanol	254.241	2.18162	2	4
Aloeresin	394.376	-0.5466	5	9
3,4-Dihydroxybenzoic acid	154.121	0.796	3	3
Aloe emodin	270.24	1.3655	3	5
1,5-Dihydroxy-3-methylanthraquinone	254.241	2.18162	2	4
7-O-Methylaloesin	408.403	-0.2436	4	9
7-O-Methylaloesinol	410.419	-0.4518	5	9

Licensed Under Creative Commons Attribution (CC BY-NC)

Feroxidin	194.23	1.5084	3	3
Nataloin	411.342	2.69792	0	2
Aloechrysone	272.3	2.4339	2	4
Aloe barbendol	258.273	2.04922	3	4
Aloenin	410.375	-0.4919	5	10
Aloesaponol I	316.309	1.83582	3	6
Aloesaponarin I	312.277	1.96822	2	6
Aloesaponol II	258.273	2.04922	3	4
Aloesaponarin II	254.241	2.18162	2	4
Isoeleutherol	244.246	2.7854	1	4
Aloesaponol IV	288.299	2.19422	3	5
Ziganein-5-methyl ether	268.268	2.48462	1	4
Pluridone	236.292	2.2892	0	4
Luteolin	286.239	2.2824	4	6
Kaempferol	286.239	2.2824	4	6
Quercetin	302.238	1.988	5	7
Oxalic acid	90.034	-0.8444	2	2
Salicylic acid	138.122	1.0904	2	2
Caffeic acid	180.159	1.1956	3	3
p-Coumaric acid	164.16	1.49	2	2
Ferulic acid	194.186	1.4986	2	3

Licensed Under Creative Commons Attribution (CC BY-NC)